Chemical Engineering Journal 229 (2013) 388–398

Contents lists available at SciVerse ScienceDirect

Chemical Engineering Journal

journal homepage: www.elsevier.com/locate/cej

Cost-effective microwave rapid synthesis of zeolite NaA for removal of methylene blue

N. Sapawe [a], A.A. Jalil [a,*], S. Triwahyono [b], M.I.A. Shah [a], R. Jusoh [a], N.F.M. Salleh [a], B.H. Hameed [c], A.H. Karim [b]

[a] Institute of Hydrogen Economy, Faculty of Chemical Engineering, Universiti Teknologi Malaysia, 81310 UTM Johor Bahru, Johor, Malaysia
[b] Ibnu Sina Institute for Fundamental Science Studies, Faculty of Science, Universiti Teknologi Malaysia, 81310 UTM Johor Bahru, Johor, Malaysia
[c] School of Chemical Engineering, Engineering Campus, Universiti Sains Malaysia, 14300 Nibong Tebal, Penang, Malaysia

HIGHLIGHTS

- NaA_{mw} was completely formed within 15 min of ageing time.
- NaA_{mw} shows better performances compared to NaA_{conv}.
- Adsorption of MB onto NaA_{mw} takes place as monolayer adsorption.
- Adsorption of MB onto NaA_{mw} was controlled by both physi- and chemi-sorption.
- NaA_{mw} was still stable after five cycling runs.

GRAPHICAL ABSTRACT

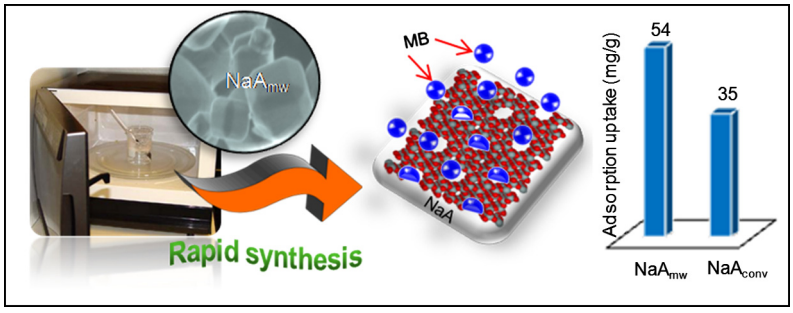

ARTICLE INFO

Article history:
Received 2 April 2013
Received in revised form 30 May 2013
Accepted 1 June 2013
Available online 11 June 2013

Keywords:
Adsorption
Methylene blue
Microwave
Zeolite NaA
Optimization

ABSTRACT

In this study, microwave rapid synthesized NaA (NaA_{mw}) was used to adsorb a methylene blue (MB) from an aqueous solution. The adsorption was optimized under four independent variables including: pH, adsorbent dosage, initial concentration, and ageing time based on central composite design (CCD) with response surface methodology (RSM). A period of 15 min was determined to be the optimum microwave ageing time for the synthesis of NaA_{mw}, which is about sixteen times shorter than using conventional heating technique. An amount of 1.0 g L^{-1} NaA_{mw} demonstrated the optimum dosage for adsorption of 120 mg L^{-1} MB, with predicted adsorption uptake of 53.5 mg g^{-1}, at pH 7 within 1 h of contact time at room temperature. This result approximated the laboratory result, which was 50.7 mg g^{-1}. The experimental data obtained with NaA_{mw} best fits the Langmuir isotherm model and exhibited a maximum adsorption capacity (q_{max}) of 64.8 mg g^{-1}, and the data followed the first-order kinetic equation. The intraparticle diffusion studies revealed that the adsorption rates were not controlled solely by the diffusion step. Thermodynamic studies showed that the adsorption is endothermic, non-spontaneous in nature, and favor at high temperature. These results confirm that the adsorption process of MB onto NaA_{mw} was controlled by both physisorption and chemisorption. The reusability study shows that the NaA_{mw} was still stable after five cycling runs. These results indicate that NaA_{mw} efficiently adsorbed MB, and could be utilized as a cost-effective alternative adsorbent for removing cationic dyes in the treatment of wastewater.

1. Introduction

The recent rapid increase in the use of the synthetic dyes, especially in the textile industry, is a major contributor to water pollution. Most of these dyes, including methylene blue, are toxic and must be removed from wastewater before discharge into water bodies, to ensure they remain safe for living organisms [1]. Adsorption on activated carbon is a popular method for removing dyes on the industrial scale [2,3]. However, activated carbon is still considered expensive and thus, much research is conducted into exploring the development of low-cost adsorbents, such as natural,

* Corresponding author. Tel.: +60 7 5535581; fax: +60 7 5536165.
E-mail address: aishah@cheme.utm.my (A.A. Jalil).

1385-8947/$ - see front matter © 2013 Elsevier B.V. All rights reserved.
http://dx.doi.org/10.1016/j.cej.2013.06.005

agricultural, and industrial byproduct waste [4–6]. Clay materials, such as: bentonite, montmorillonite, kaolinite, and zeolite [7–13] have received much consideration due to their unique structural and surface properties, which offer high chemical stability and specific surface area that leads to high adsorption capacities [14]. Of these clays, zeolite has received the greatest attention and recognition as a good adsorbent.

NaA zeolite is an aluminosilicate with a small pore size of 4 Å, has a unit cell formula of $Na_{12}[(AlO_2)_{12}(SiO_2)_{12}]\cdot 27H_2O$ and a crystalline structure, which is generally synthesized by a heating method, such as in situ hydrothermal synthesis or secondary growth [15–17]. Recently, a technique of NaA synthesis using microwave heating has been intensely studied due to its rapid and uniform heating that leads to a short crystallization time and homogeneous nucleation [16–18]. The unique framework and high cation exchange capacity of NaA make it able to adsorb various gaseous and heavy metal ions [17,18]. However, the report of NaA on adsorption of dyes is still in a nascent stage. Therefore, in this study we report an efficient removal of methylene blue dye using microwave rapid synthesized NaA. The microwave synthesis time was shortened by sixteen times compared with the conventional method. The detailed objectives of our investigation were: (i) to prepare the NaA by microwave technique and to compare its properties with NaA synthesized by conventional method (NaA_{conv}) using X-ray diffraction (XRD), field emission scanning electron microscopy coupled with energy dispersive X-ray (FE-SEM/EDX), and Brunnauer–Emmett–Teller surface area analysis (BET); (ii) to study the feasibility of NaA_{mw} as an adsorbent for MB dye, and optimize the adsorption using a central composite design-based (CCD) response surface methodology (RSM) under four independent variables including pH, adsorbent dosage, initial concentration, and ageing time; (iii) to determine the applicability of various isotherm models (i.e., Langmuir, Freundlich, Temkin, and Dubinin–Radushkevich) to establish the best-fit isotherm equation; (iv) to evaluate the usefulness of various kinetic models (i.e., pseudo-first-order, pseudo-second-order, and intraparticle diffusion models); (v) to study the thermodynamic properties (free Gibbs energy, enthalphy, and entrophy); and (vi) to study the reusability of the NaA_{mw}.

2. Material and methods

2.1. Materials

Colloidal silica (30% SiO_2 and 0.32% Na_2O, Ludox HS-30), sodium aluminate (Sigma–Aldrich Laborchemikalien GmbH), and sodium hydroxide pellets (Grade AR, QReC™) were used as received. Sodium hydroxide (NaOH), hydrochloric acid (HCl), and methylene blue (C.I. 52015 for microscopy) were obtained from QReC™. All reagents were of analytical grade and were used as received. Deionized water was used for the preparation of the pH solution and adjustments to the pH were performed using a 0.1 M HCl and NaOH solution.

2.2. Preparation of NaA

The colloidal solution used for the synthesis of NaA by both hydrothermal and microwave methods was prepared as follows: Solution *A* was prepared by dissolving 1.88 g of NaOH in 75 mL deionized water and mixed with 2.4 mL of Ludox. Solution *B* was prepared by dissolving 5.64 g NaOH in 25 mL of deionized water and mixed with 7.12 g of $NaAlO_2$. Both of the solutions were prepared at room temperature and stirred vigorously for 10 min. Then, these two solutions (*A* and *B*) were mixed together for 1 h at 368 K to give a clear homogeneous solution. The molar composition of the resulting colloidal solution was: 1.0 Al_2O_3:1.96 SiO_2:3.165 Na_2O:128 H_2O.

For the hydrothermal method (NaA_{conv}), the solution of mixed *A* and *B* was transferred into a 100 mL Teflon vessel and placed in an oven at 378 K for 4 h, prior to being filtered and washed until the solution pH < 9. For the microwave method (NaA_{mw}), the 100 mL Teflon vessel containing the mixture of solutions *A* and *B* was radiated in a conventional microwave (100 W) for 15 min and then received the same work-up procedure as in the hydrothermal method. Both of the crude catalysts were oven dried overnight at 378 K before being calcined at 823 K for 3 h to produce a white powder of NaA.

2.3. Characterization of NaA

The NaA were characterized using differential analytical techniques. The XRD patterns of the NaA were obtained and recorded on a D8 ADVANCE Bruker X-ray diffractometer using Cu Kα radiation at a 2θ angle ranging from 3° to 90°. The phases were identified with the aid of the Joint Committee on Powder Diffraction Standards (JCPDS) files. The topological properties as well as semi-quantitative determination were observed by field emission scanning electron microscopy coupled with energy dispersive X-ray spectrometer (FE-SEM/EDX) (JSM-6701F). FTIR (Perkin Elmer Spectrum GX FTIR Spectrometer) was performed using the KBr method with a scan range of 400–4000 cm^{-1}. The specific surface area was determined from nitrogen adsorption–desorption isotherms at the temperature of liquid nitrogen using a Micromeritics ASAP 2010 instrument. The surface area was calculated with the BET method. Prior to measurement, all the samples were degassed at 383 K to 0.1 Pa. The absorbance measurement of the dye decolorization was monitored by a double-beam UV–vis spectrophotometer (Agilent Technologies Cary 60 UV–vis).

2.4. Adsorption experiments

Adsorption experiments were performed by adding 0.05 g of NaA to a 100 mL conical flask containing 50 mL of a 10 mg L^{-1} methylene blue (MB) solution under pH 7 for 1 h at room temperature (303 K). The pH of the working solution was adjusted to the desired value with HCl or NaOH. The mixtures were prepared under constant stirring at a rate of 300 rpm at room temperature (303 K) to reach equilibrium. The samples were then withdrawn at appropriate time intervals and centrifuged at 3500 rpm for 15 min. The residual MB concentration was determined using a UV–vis spectrophotometer at 664 nm. At any time, *t*, the adsorption capacity of MB adsorbed (q_t) and the removal percentage of MB onto NaA was calculated by the following mass-balance equation:

$$\text{Adsorption uptake/capacity}(\text{mg g}^{-1}): q_t = \frac{(C_o - C_t)V}{W} \quad (1)$$

$$\text{Removal}(\%): \left(\frac{C_o - C_t}{C_t}\right) \times 100 \quad (2)$$

where C_0 and C_t (mg L^{-1}) are the liquid-phase concentrations of dye at time zero and at time *t*, respectively. *V* (L) is the volume of the solution and *W* (g) is the mass of NaA used.

2.5. Experimental design and optimization (DOE)

The effects of the operating parameters were optimized using response surface methodology (RSM). RSM is a set of mathematical and statistical methods for: designing experiments, constructing models, evaluating the effects of variables, and seeking optimum conditions of variables to predict targeted responses. It also can determine a region where the factors of a certain operating specification are met. The application of statistical experimental design techniques in adsorption processes could result in: improved

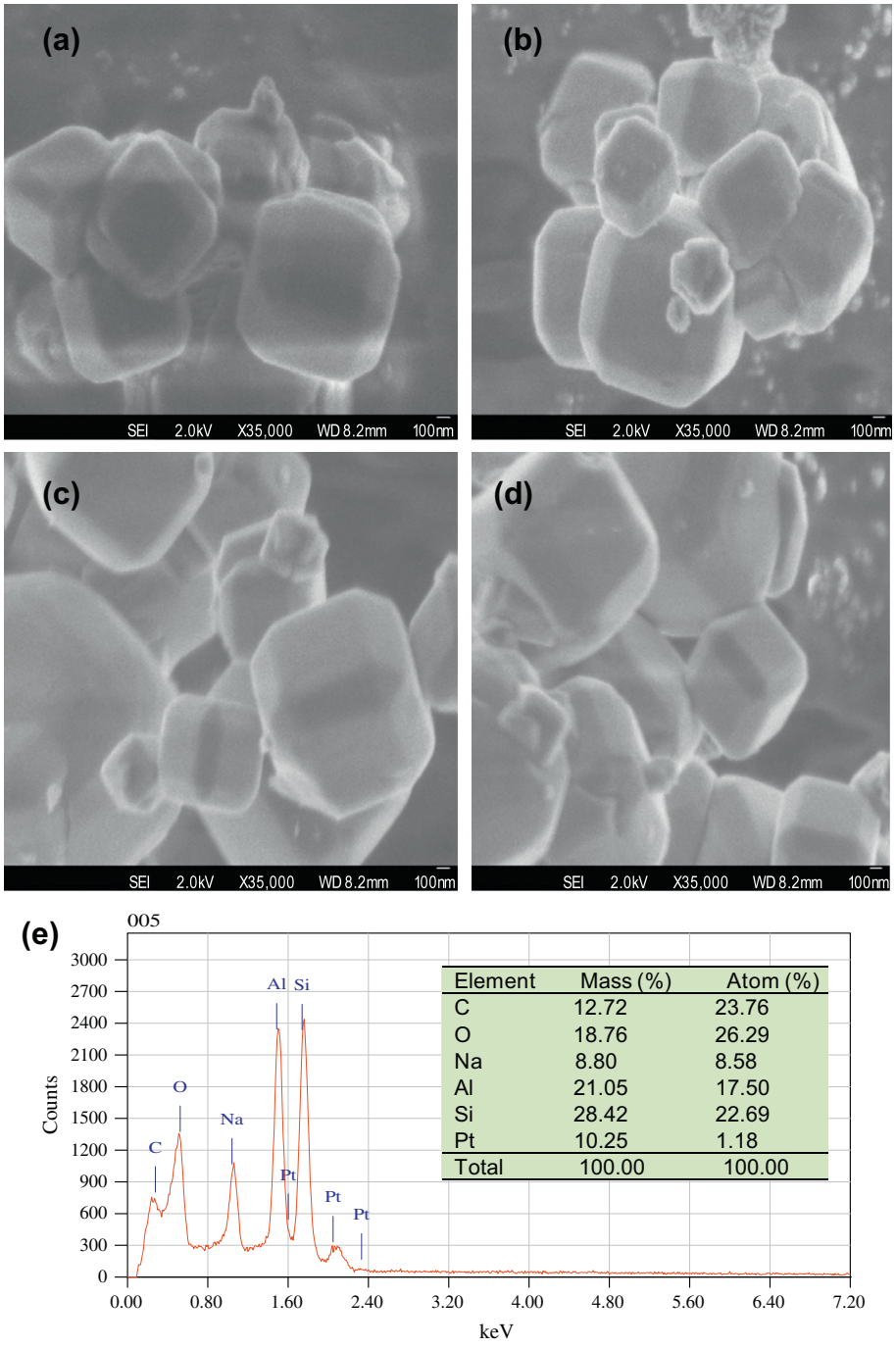

Fig. 1. FE-SEM images of NaA zeolite prepared by (a) conventional method, and microwave at (b) 5 min, (c) 10 min, (d) 15 min and (e) The EDX analysis of elemental composition of NaA_{mw}.

adsorptive capability, reduced process variability, closer confirmation of the output response to nominal and targeted requirements, as well as reduced development time and overall costs [19]. In this paper, central composite design (CCD) was chosen for the RSM in the experimental design, which is appropriate for fitting a quadratic surface and usually works well for process optimization. The CCD is an effective design that is ideal for sequential experimentation and allows a reasonable amount of information for testing lack of fit, whilst not involving an unusually large number of design points [20]. Therefore, central composite non-factorial surface design with four factors was applied using Statistica 6.0 StatSoft without any blocking. The bounds of the factors are initial pH: 5–9, adsorbent dosage: 1–10 g L^{-1}, initial concentration: 10–120 mg L^{-1}, and ageing time: 5–15 min, and were chosen based on the results of preliminary studies that have been conducted. The performance of the adsorption was evaluated by analyzing the response of the affinity of NaA_{mw} for the MB. The adsorption uptake of the affinity of NaA_{mw} was chosen as the response value.

3. Results and discussion

3.1. Characterization of the adsorbent material

FE-SEM images show a cubic-type crystalline structure with a well-defined edge of the NaA particles (Fig. 1). The structures of

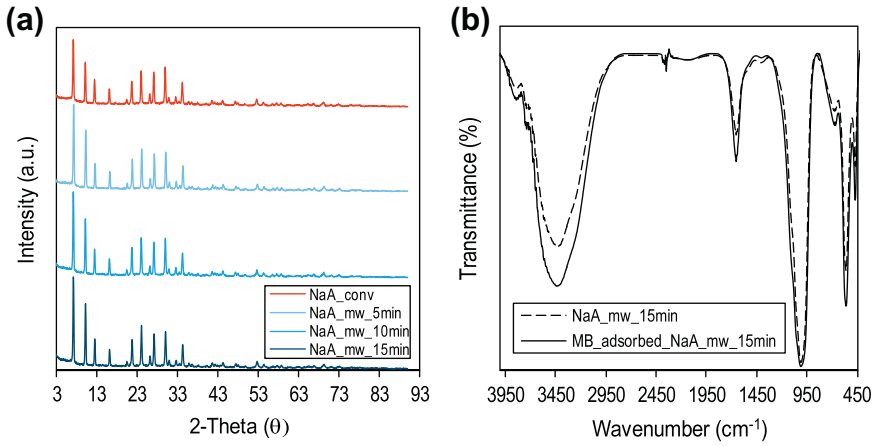

Fig. 2. (a) XRD patterns of NaA zeolite prepared by conventional method and microwave at 5 min, 10 min, 15 min and (b) FTIR spectra of NaA_{mw} and MB adsorbed NaA_{mw}.

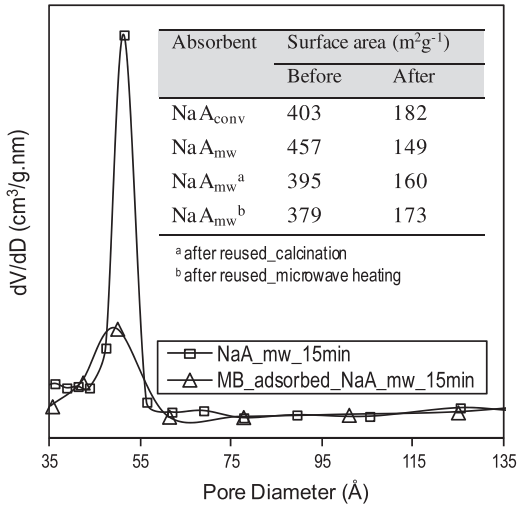

Absorbent	Surface area (m^2g^{-1})	
	Before	After
NaA_{conv}	403	182
NaA_{mw}	457	149
NaA_{mw}[a]	395	160
NaA_{mw}[b]	379	173

[a] after reused_calcination
[b] after reused_microwave heating

Fig. 3. Pore size distribution curves of NaA_{mw} and MB adsorbed NaA_{mw} and the inset table is the specific surface area analysis of NaA zeolite.

NaA_{conv} (Fig. 1a) are similar to those of NaA_{mw} (Fig. 1b–d), but NaA_{mw} radiated for 15 min in a microwave (Fig. 1d) shows more complete formation of NaA (cubic-type crystal). From the analysis, we can estimate that the particle size of the product was around 0.2–2 μm. The symmetrical and uniform size of NaA is expected to provide high active sites and thus, allow the dye's molecules to easily adsorb onto the surface [21]. The EDX analysis (semi-quantitative) was employed to determine the composition of the NaA_{mw} (Fig. 1e). The peaks of Na, Al and Si were corresponded to zeolitic product, whereas Pt and C originated from the coated material as well as the platform of the holder sample. No other element was detected, indicating that NaA_{mw} is free from other impurities.

The XRD patterns of the prepared NaA were compared for both NaA_{conv} and NaA_{mw}, and the results are shown in Fig. 2a. The peak intensity of NaA_{mw} increased as the time of microwave irradiation was increased. A series of characteristic peaks were observed at: 7.2° (200), 10.1° (220), 12.4° (222), 16.1° (420), 21.6° (600), 23.9° (622), 27.1° (642), 30.0° (644) and 34.1° (640), which was in agreement with the JCPDS data of card No. 39-0222 [21]. However, no other diffraction peaks were detected, indicating the purity of the prepared NaA.

FTIR spectroscopy is a very useful technique for obtaining vibrational information about the species in materials. Therefore, NaA_{mw} and MB absorbed NaA_{mw} were subjected to FTIR analysis and the results are shown in Fig. 2b. Several characteristic bands are observed: those at 1022 cm^{-1} correspond to the internal vibration of (Si, Al)–O asymmetric stretching; those at 564 cm^{-1} correspond to the external vibration of double four-rings; those at 689 cm^{-1} correspond to the internal vibration of (Si, Al)–O symmetric stretching; and those at 467 cm^{-1} correspond to the internal vibration of (Si, Al)–O bending. The band related to OH also appeared at about 1653 cm^{-1} [21,22]. A broad absorption peak was observed at 3475 cm^{-1}, which was assigned to the OH stretching vibration in the hydroxyl groups. The increase in intensity of OH stretching vibration at 3475 and 1653 cm^{-1} after adsorption, suggests the possibility that an interaction occurred between the NaA_{mw} and MB.

The surface area analysis data obtained from the BET method can be used to verify this result (inset table in Fig. 3). The decrease in NaA_{mw} surface area after adsorption signifies that MB was attracted towards the NaA_{mw} surface, via hydrogen bonding or electrostatic interaction. However, this phenomenon led to a high concentration of MB on the NaA_{mw} surface, resulting in pore blockage and thus, reduces the surface area of NaA_{mw} and decreases the adsorption activity due to saturation, as well as contamination of the NaA_{mw} surface. The adsorption of MB onto the NaA_{mw} surface was also confirmed by the pore blockage, which is shown in Fig. 3.

3.2. Response surface modeling

As there only have three levels for each factor, the appropriate model is the quadratic model as below,

$$Y = \beta_0 + \sum_{j=1}^{k}\beta_j X_j + \sum_{j=1}^{k}\beta_{jj} X_j^2 + \sum_{i<j}^{k}\beta_{ij} X_i X_j \quad (3)$$

where Y = response, X_i and X_j = variables, β_0 = constant coefficient, β_j, β_{jj}, and β_{ij} = interaction coefficients of linear, quadratic and second-order terms, respectively, and k is the number of studied factors. The quality of the fit of polynomial model was expressed by the value of correlation coefficient (R^2). The main indicators demonstrating the significance and adequacy of the model used include the model F-value (Fisher variation ratio), and P-value (Probability value) [23].

3.2.1. Experimental design and quadratic model

Four factors: the pH, adsorbent dosage (AD), initial concentration (IC), and ageing time (AT) have been optimized by RSM using Statistica 6.0 StatSoft for removal of MB by NaA_{mw}. The list of experiments designed by RSM and the value of response (adsorption

uptake, mg g^{-1}) for each sample obtained for the corresponding experimental conditions, are shown in Table 1. The regression analysis was performed to fit the response, and the final regression function for response in terms of the coded factors used in generating the statistical model is given below:

$$\begin{aligned} Y(\text{adsorption capacity, mg g}^{-1}) = {} & -1.83786 + 2.25428X_{pH} \\ & - 4.25352X_{AD} + 0.45268X_{IC} \\ & - 0.24208X_{AT} - 0.01643X_{pH}X_{AD} \\ & + 0.00374X_{pH}X_{IC} \\ & + 0.04015X_{pH}X_{AT} \\ & - 0.03762X_{AD}X_{IC} \\ & - 0.02575X_{AD}X_{AT} \\ & + 0.00122X_{IC}X_{AT} - 0.18787X_{pH}^2 \\ & + 0.41518X_{AD}^2 - 0.00084X_{IC}^2 \\ & + 0.00692X_{AT}^2 \end{aligned}$$

Table 2 shows the analysis of variance (ANOVA) of the regression parameters of the predicted response surface quadratic model. Because the model value $F = 27.8791$ exceeded the table value $F_{(14,11,0.05)} = 2.7186$ and a low probability value ($P > F < 0$), the Fisher F-test demonstrated that the experimental results fitted well and indicates that the model was significant. In addition, the values of $P > F$ less than 0.05 indicate that the model terms are significant, while values greater than 0.10 indicate that the model terms are not significant [23].

Table 1
Experimental design and response value for different conditions at 60 min.

Run no.	Factor				Response (adsorption uptake)	
	X_{pH} pH	X_{AD} Adsorbent dosage (g L^{-1})	X_{IC} Initial concentration (mg L^{-1})	X_{AT} Ageing time (min)	Actual (mg g^{-1})	Predicted (mg g^{-1})
1	5	1	10	5	4.73	4.97
2	5	1	10	15	4.86	5.80
3	5	1	120	5	37.1	36.2
4	5	1	120	15	38.4	38.2
5	5	10	10	5	0.994	2.51
6	5	10	10	15	0.962	1.02
7	5	10	120	5	4.04	3.30
8	5	10	120	15	3.62	2.91
9	9	1	10	5	3.75	4.35
10	9	1	10	15	5.66	6.79
11	9	1	120	5	36.9	37.0
12	9	1	120	15	42.4	40.5
13	9	10	10	5	0.991	1.30
14	9	10	10	15	0.951	1.42
15	9	10	120	5	4.46	3.43
16	9	10	120	15	4.48	4.65
17	5	5	50	10	5.34	5.10
18	9	5	50	10	5.43	5.62
19	7	1	50	10	22.2	22.2
20	7	10	50	10	4.75	4.72
21	7	5	10	10	1.29	3.99
22	7	5	120	10	9.73	15.0
23	7	5	50	5	5.81	5.74
24	7	5	50	15	6.81	6.83
25		(C)	7	5		
					50	10
6.03		6.11	26 (C)	7		
					5	50
		6.03	6.11			
10						

*Contact time and temperature were constant at 1 h and 303 K, respectively.

Table 2
ANOVA for analysis of variance and adequacy of the quadratic model.

Source	Sum of squares	Degree of freedom	Mean square	F-value	Prob > F
X_{AD}	1650.42	1	1650.42	271.23	0.000000
X_{AD}^2	176.27	1	176.27	28.97	0.000223
X_{IC}	1337.96	1	1337.96	219.88	0.000000
$X_{AD}X_{IC}$	930.95	1	930.95	152.99	0.000000
Regression	4121.90	14	294.42	27.88	–
Residual	116.17	11	10.56	–	–
Total	4238.07	25	–	–	–

*F-value (27.8791) calculated > F-value (2.7186) from F-table.
*$R^2 = 0.9842$; $R^2_{adj} = 0.9641$.

3.2.2. Effects of model components and their interactions on dye adsorption

To study the interaction between all four factors, three-dimensional response surface curves were plotted. The combined effect of IC and AD on the adsorption uptake of NaA_{mw} (mg g^{-1}) is shown in Fig. 4a as response surface plots and Fig. 4b as contour plots. The adsorption uptake increased up to 53.5 mg g^{-1}, with increased IC and decreased AD. In contrast, pH and AT did not show any interaction between either IC or AD. In addition, when pairing these two factors with respect to IC and/or AD, a flat response surface plot was produced indicating that pH (Fig. 4c and e) and AT (Fig. 4d and f) had no significant effect on adsorption uptake of NaA_{mw} (mg g^{-1}). The pareto chart also verified that IC and AD were the most significant factors affecting the adsorption uptake of NaA_{mw} (Fig. 5).

3.2.3. Model validation

The mathematical model generated during RSM implementation was validated by conducting experiments for a given optimal medium setting. An amount of 1.0 g L^{-1} NaA_{mw} was found to be the optimum dosage for 120 mg L^{-1} MB, with predicted adsorption uptake of 53.5 mg g^{-1}, at pH 7 using 15 min ageing time NaA_{mw}. The experiment was conducted based on these appropriate conditions to confirm the actual value. The laboratory results gave 50.7 mg g^{-1}, which is very close and fitted well with the optimized value generated by the RSM tools. The experimental measurements show that NaA_{mw} gave better performance compare with NaA_{conv} (Table 3). It was suggested that a high surface area (inset table in Fig. 3) was activated when applying microwave radiation to NaA_{mw}, which results in high adsorption uptake. The appropriate conditions generated by RSM were taken into consideration and were used for further studies on adsorption equilibrium isotherms, kinetics, and thermodynamics.

3.3. Adsorption equilibrium studies

In this study, the equilibrium experimental data were fitted with four commonly used isotherm models: the Langmuir, the Freundlich, the Temkin and the Dubinin–Radushkevich, to describe the interaction between the MB molecules and the surfaces of the NaA_{mw}, and to analyze the distribution type of MB in the liquid and solid phases [24–26]. Identification of the best-fit isotherm model is essential for optimization of the adsorption process design. The non-linear regression of those isotherm models can be represented by the expression [27],

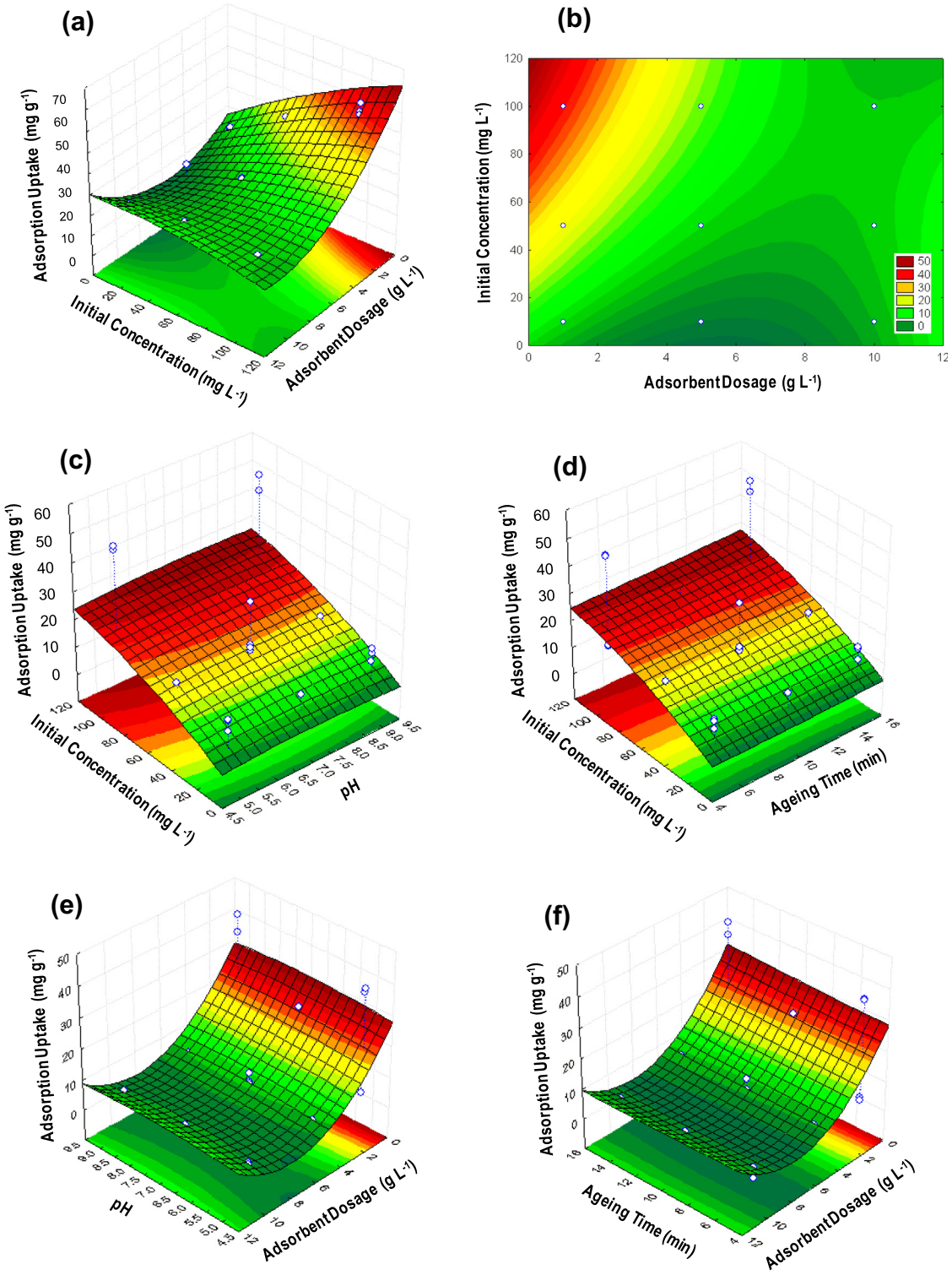

Fig. 4. Response surface plots for adsorption uptake of NaA_{mw} showing interaction between (a) initial concentration and adsorbent dosage (c) initial concentration and pH (d) initial concentration and ageing time (e) adsorbent dosage and pH (f) adsorbent dosage and ageing time, and (b) contour plots for adsorption uptake of NaA_{mw} as a function of initial concentration and adsorbent dosage (1 h contact time).

$$\text{Langmuir isotherm}: \quad q_e = \frac{q_m K_L C_e}{1 + K_L C_e} \tag{4}$$

$$\text{Freundlich isotherm}: \quad q_e = K_F C_e^{1/n_F} \tag{5}$$

$$\text{Temkin isotherm}: \quad q_e = B \ln(AC_e) \tag{6}$$

$$\text{Dubinin–Radushkevich(D–R)}: \quad q_e = q_m \exp(-K_{DR}\varepsilon^2) \tag{7}$$

$$\varepsilon = RT \ln(1 + 1/C_e)$$

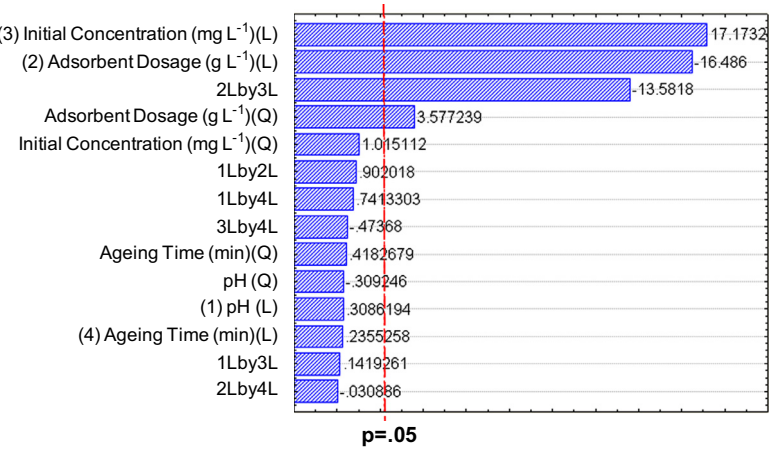

Fig. 5. Pareto chart of standardized effect estimate (absolute value).

Table 3
Optimization results of adsorption uptake NaA zeolite.

Preparation method	Adsorption uptake (mg g^{-1})
Predicted by RSM model	53.5[a]
Microwave	50.7[a]
Conventional	34.7[b]

pH 7; 1.0 g L^{-1} NaA; 120 mg L^{-1} MB.
[a] 15 min.
[b] 4 h ageing time.

where C_e is the MB concentration at equilibrium (mg L^{-1}), q_e is the adsorption capacity at equilibrium (mg L^{-1}), q_m is the maximum adsorption capacity (mg L^{-1}), K_L is the Langmuir constant (mg L^{-1}), K_F is the Freundlich adsorbent capacity, n_F is the heterogeneity factor, A is the Temkin equilibrium binding constant (L g^{-1}), B is the Temkin constant, K_{DR} is D–R constant (mol^2 kJ^{-2}), ε is the Polanyi potential (J mol^{-1}), R is gas constant (8.314 J mol^{-1} K^{-1}), and T is absolute temperature (K).

The plots of these isotherm models are illustrated in Fig. 6a and all of their coefficients are listed in Table 4. The essential characteristics of the Langmuir isotherm can be expressed in term of the dimensionless constant separation factor, R_L, which is given by the following equation:

$$R_L = \frac{1}{1 + K_L C_0} \tag{8}$$

The R_L parameter is considered a more reliable indicator of the adsorption [28], which indicates the shape of the isotherm to be either unfavorable ($R_L > 1$), linear ($R_L = 1$), favorable ($0 < R_L < 1$), or irreversible ($R_L = 0$).

The Langmuir was observed to be the best-fit model for the experimental data due to the highest regression coefficient ($R^2 = 0.999$) compared with the other isotherm models. This result suggests that the adsorption of MB onto the surface of NaA$_{mw}$ takes place as monolayer adsorption. The R_L value was 0.219, which indicates that the adsorption is a favorable process. The correlation coefficient of the Temkin model was also high ($R^2 = 0.994$), which indicates good linearity. The Temkin adsorption potential (B ln A) was 16.4 kJ mol^{-1}, illustrating that the bond between the MB molecules and the NaA$_{mw}$ is quite weak [29]. In addition, the E value represented by the D–R isotherm was 0.129 kJ mol^{-1}, which is in the range of the physisorption process [30]. Thus, these results confirm that the adsorption of MB onto NaA$_{mw}$ was controlled by the physisorption process.

3.4. Comparison of NaA with other adsorbents

Other researchers have also reported a Langmuir model for the adsorption of cationic dyes [31]. As shown in Table 5, the maximum adsorption capacity (q_m) of NaA$_{mw}$ for MB is comparable, and was found to be the higher than that of many corresponding adsorbents reported in the literature [31–45]. According to the results obtained, NaA$_{mw}$ has a potential to be employed as a cost-effective adsorbent and could be considered as an alternative to commercial activated carbons for the removal of color.

3.5. Kinetic studies

It is important to study the adsorption kinetics in the treatment of aqueous effluent because it provides valuable information on the efficiency and mechanism of the adsorption process. Three commonly used models to describe the adsorption behavior of pollutants on solid surfaces are the pseudo-first-order, pseudo-second-order and intraparticle diffusion models [25,46]. The non-linear forms of pseudo-first and -second order, and linear form of intraparticle diffusion models are given as:

$$\text{Pseudo-first-order equation}: \quad q = q_e(1 - e^{-k_1 t}) \tag{9}$$

$$\text{Pseudo-second-order equation}: \quad q = \frac{q_e^2 k_2 t}{1 + q_e k_2 t} \tag{10}$$

$$\text{Weber—Morris equation}: \quad q_t = k_{id} t^{1/2} C \tag{11}$$

For the non-linear regression method, the experimental data of the dye uptake, q, versus time, t, were fitted to those models by using the *solver* add-in with Microsoft's Excel spreadsheet (Microsoft) and the results are shown in Fig. 6b [47]. Table 6 lists their rate constants (k_1 and k_2) and the corresponding linear regression correlation coefficient values (R^2). At all the initial concentrations studied, the values of R^2 for the pseudo-first-order model were greater ($R^2 = 0.999$), and the theoretical $q_{e.calc}$ values obtained from this model were also closer to the experimental $q_{e,exp}$ compared with the values obtained from the pseudo-second-order model. These results indicate that the adsorption of MB onto NaA$_{mw}$ could be better explained based on the pseudo-first-order kinetics model, and this result is in agreement with the isotherm data, verifying that the adsorption occurred through a physisorption process [24].

The plots of the intraparticle diffusion model of Weber–Morris at different initial concentrations are shown in Fig. 6c. It seems that the plots are separated into three steps for low concentrations of MB at 5 and 10 mg L^{-1}, two steps for 40 mg L^{-1}, and become linear

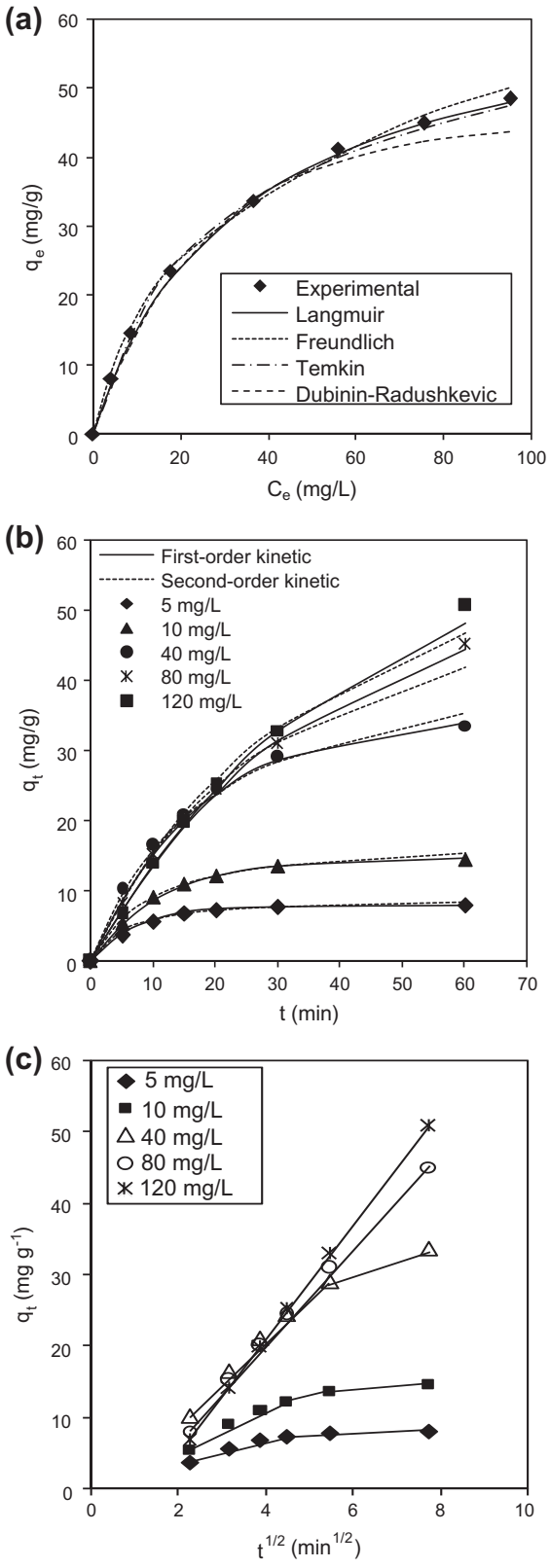

Fig. 6. (a) Equilibrium isotherm (Langmuir, Freundlich, Temkin, Dubinin–Radushkevich model); (b) Pseudo-first order and pseudo-second order kinetic models; and (c) Intraparticle diffusion model of adsorption of MB removal onto NaA_{mw} (pH = 7, AD = 1.0 g L^{-1}, IC = 120 mg L^{-1}, AT = 15 min, t = 1 h, 303 K).

for high concentrations of 80 and 120 mg L^{-1} of MB. However, the linear plots did not pass through the origin, suggesting that intraparticle diffusion is not the only rate-determining step for those concentrations [28]. The plots became sharper with an increase in initial concentrations, illustrating the increase in the rate of adsorption (Table 6). The final stage of the 5 and 10 mg L^{-1} plots exhibit a slowdown demonstrating that equilibrium was achieved as most of the adsorption sites became saturated. At lower concentrations, higher numbers of available active sites on the NaA_{mw} surface may allow the MB molecules to be adsorbed slowly with multi-steps of reactions, involving the diffusion of MB from the external liquid-film boundary layer to the external NaA_{mw} surface sites. This is then followed by the intraparticle diffusion of MB within the pores of the NaA_{mw} and finally, the attachment of MB onto the NaA_{mw} at available adsorption sites [46]. However, at high concentrations, the interaction between the large number of MB ions in the solution and limited active sites on the NaA_{mw} surface may occur rapidly, and the first and third steps of the process could be neglected. Therefore, the linear lines at high concentrations may correspond to the intraparticle diffusion of MB ions within the pores. These kinetics results verify that the adsorption is a physisorption process.

Table 4
Isotherm parameters for removal of MB on NaA_{mw}.

Isotherm	Parameters	Values
Langmuir	q_m (mg g^{-1})	64.8
	K_L (L mg^{-1})	2.97×10^{-2}
	R^2	0.999
	R_L	0.219
Freundlich	K_F	6.55
	n	2.22
	R^2	0.975
Temkin	A (L mg^{-1})	0.310
	B	14.0
	R^2	0.994
Dubinin–Radushkevich	q_m (mol g^{-1})	39.6
	B (mol^2 J^{-2})	3.0×10^{-5}
	R^2	0.948
	E ($1/\sqrt{2\beta}$) (kJ mol^{-1})	0.129

Table 5
Comparison of maximum adsorption capacities of various adsorbents for methylene blue.

Adsorbent	Maximum adsorption capacity (mg g^{-1})	Ref.
NaA_{mw}	64.8	*This work*
Zeolite fly ash (ZFA)	14.3	[32]
Silica	11.2	[33]
Fly ash	1.30	[33]
Pure kaolin	15.6	[34]
Clay	58.2	[31]
Coir pith carbon	5.87	[35]
Acid activated carbon	60.6	[36]
Activated carbon	109	[37]
Activated olive stone	16.1	[38]
Activated sewage char	12.0	[39]
Chrome sludge	0.51	[40]
Coffee husks	90.1	[41]
Lemon peel	29.0	[42]
Banana peel	20.8	[43]
Yellow passion fruit waste	44.7	[44]
Luffa cylindrical fibers	47.0	[45]

3.6. Thermodynamics studies

Thermodynamics parameters were evaluated to investigate the nature of the adsorption. The effect of temperature on the adsorption of MB onto NaA_{mw} was studied over the temperature range of

Table 6
Kinetic parameters for the adsorption of MB onto NaA_{mw} at different initial concentrations.

C_0 (mg L^{-1})	$q_{e,exp}$ (mg g^{-1})	Pseudo-first-order kinetic model			Pseudo-second-order kinetic model			Intraparticle diffusion		
		$k_1 \times 10^{-2}$ (min^{-1})	$q_{e.cal}$ (mg g^{-1})	R^2	$k_2 \times 10^{-4}$ (g mg^{-1} min^{-1})	$q_{e.cal}$ (mg g^{-1})	R^2	k_{id} (mg g^{-1} $min^{0.5}$)	C	R^2
5	8.04	12.4	8.09	0.999	8.87	8.87	0.996	0.713	3.39	0.719
10	14.6	8.99	14.0	0.999	16.9	16.9	0.996	1.55	4.03	0.818
40	33.6	6.45	32.9	0.999	42.6	42.6	0.998	4.20	3.61	0.927
80	45.1	3.68	44.3	0.999	75.8	75.8	0.996	6.67	5.97	0.998
120	50.7	3.45	52.7	0.999	112.4	112	0.975	7.99	11.0	0.999

Table 7
Thermodynamic parameters for the adsorption of MB onto NaA_{mw}.

Temp (K)	q_e (mg g^{-1})	$K_c \times 10^{-2}$	ΔG^o (kJ mol^{-1})	ΔH^o (J mol^{-1})	ΔS^o (J mol^{-1} K^{-1})
303	50.7	4.42	7.86		
323	100	9.13	6.43	34.5	87.7
343	216	22.0	4.32		

303–343 K. The thermodynamics parameters, including the free Gibbs energy (ΔG^o), enthalpy (ΔH^o) and entrophy (ΔS^o) were calculated using the equations below:

$$\text{Free energy change}: \quad \Delta G^0 = -RT \ln K_C \tag{12}$$

$$\text{Equilibrium constant}: \quad K_C = \frac{C_e(adsorbent)}{C_e(solution)} \tag{13}$$

$$\text{van't Hoff equation for enthalpy and entrophy}: \quad \ln K_C = \frac{\Delta S^O}{R} - \frac{\Delta H^O}{RT} \tag{14}$$

The values of the thermodynamics parameters obtained are listed in Table 7. It was observed that the adsorption capacity of the MB increased with increasing temperature, indicating the process was endothermic. A positive sign and a decrease in the magnitude of overall standard free energy change with an increase in the temperature, indicates that the process was non-spontaneous in nature and favor at high temperature, respectively [48]. The positive value of ΔH^o confirms the endothermic nature of the overall adsorption process, and its magnitude (34.5 J mol^{-1}) below 20.9 kJ mol^{-1} is in the heat range of the physisorption process [49]. This fact was in agreement with the isotherm and kinetic experiments. However, the adsorption process may also involve both physisorption and chemisorption due to the endothermic nature of the system [50]. At higher temperatures, the surface activity and kinetic energy of MB were increased, which results in more available active sites on the NaA_{mw} surface to enhance the adsorption of MB. The positive value of ΔS^o (87.7 J K^{-1} mol^{-1}) corresponds to an increase of the randomness at the solid-solute interface, and suggests good affinity of MB toward the NaA. Similar findings were also reported in [6,28].

3.7. Regeneration study

A repeat experiment was performed with NaA_{mw} to study the stability of the NaA_{mw} for MB decolorization (Fig. 7). The initial concentration of MB was maintained constant (10 mg L^{-1} and 100 mg L^{-1}) at pH 7 for 1 h of contact time, and the NaA_{mw} was recycled after filtration before undergoing two different methods of treatment, via calcination at 823 K for 3 h and/or microwave heating at 300 W for 15 min, at every cycle. It can be observed that after five repeated experiments, the NaA_{mw} was still active which shown by a slightly decrease in decolorization percentage of 10 mg L^{-1} MB with 7.1% and 17.3% for calcination and microwave heating, respectively. Similar trend was also observed for 100 mg L^{-1} MB with only 5.6% and 12.5% of decolorization percentage drop for the former and latter treatment, respectively. It is suggested that the heat treatment most probably induced NaA_{mw} aggregation after several recycles, which resulted in a decrease of surface area (inset table in Fig. 3), and subsequently led to a decrease in decolorization efficiency [51–55].

3.8. Energy and cost estimation

Energy and cost estimation is a well formulated prediction of the probable production cost to propose a specific budget of material used. In this study, the total energy and cost that were consumed for the production of approximately 5.0 g per batch NaA zeolite was estimated and listed in Table 8. It could be observed that the microwave synthesis time was shortened by 16 times

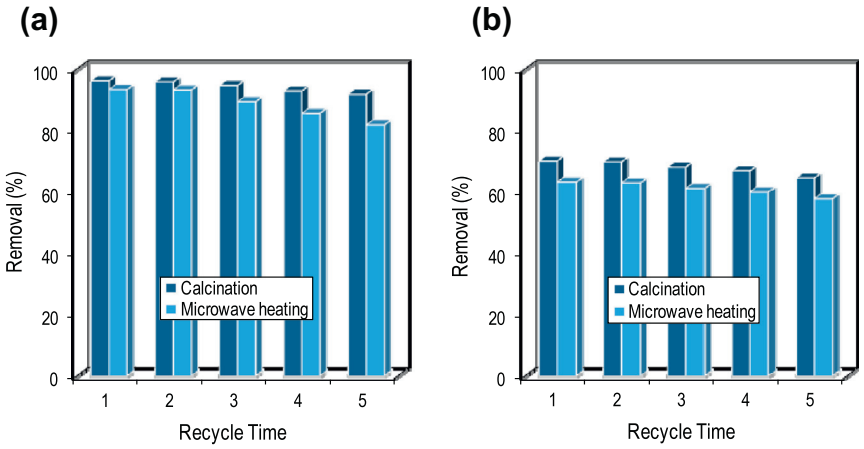

Fig. 7. The reusability of adsorption of MB removal onto NaA_{mw} (pH = 7, AD = 1.0 g L^{-1}, IC = 10 mg L^{-1} and 100 mg L^{-1}, AT = 15 min, t = 1 h, 303 K).

Table 8
Energy and cost estimation for the production of NaA zeolite.

Factor	NaA_{mw}	NaA_{conv}
Time consumed (min)	15	240
Power (W)	100	2000
Total cost ($USD)	0.003	1.16

*Malaysia tariff rates of electricity, $0.14 USD/kW h.

and used 20 times less energy compared to the conventional method. The estimated electricity cost for production of NaA_{mw} is totally far cheaper than NaA_{conv}. Similar economical preparation of adsorbent was reported by Shah et al. emphasizing the low cost consumption in converting waste to useful material [56]. Both above findings lead to potential cost-effective adsorbents for removing dyes from industrial wastewater, which contribute in low-energy and -cost consumption for green sustainability.

4. Conclusions

The present study investigated the adsorption of MB from aqueous solutions by using microwave rapid synthesized NaA (NaA_{mw}). NaA_{mw} has been demonstrated to be highly effective within 1 h of contact time at room temperature. The best-fit adsorption isotherm was achieved with the Langmuir model, indicating that adsorption occurs by monolayer coverage. The positive enthalpy change for the adsorption process confirms the endothermic nature of the adsorption. The kinetic calculations show that the adsorption followed the pseudo-first-order model with a multi-step diffusion process. These results finally confirm that the adsorption of MB onto NaA_{mw} is controlled by both physisorption and chemisorption process. In addition, the laboratory results (50.7 mg g^{-1}) obtained were closer and fitted well with the optimized value given by the RSM analyzes (53.5 mg g^{-1}).The reusability study shows that the NaA_{mw} was still stable after five cycling runs. The cost-effective and abundance of NaA_{mw} make this material particularly promising for the removal of cationic dyes in industrial wastewater treatment.

Acknowledgements

The authors are grateful for the financial support by the Research University Grant from Universiti Teknologi Malaysia (Grant No. 01H59), the awards of UTM Zamalah Scholarship (Norzahir Sapawe) and the Hitachi Scholarship Foundation for their support.

References

[1] E.N. El-Qada, S.J. Allen, G.M. Walker, Adsorption of methylene blue onto activated carbon produced from steam activated bituminous coal: a study of equilibrium adsorption isotherm, Chem. Eng. J. 124 (2006) 103–110.
[2] T. Robinson, G. McMullan, R. Marchant, P. Nigam, Remediation of dyes in textile effluent: a critical review on current treatment technologies with a proposed alternative, Bioresour. Technol. 77 (2001) 247–255.
[3] E.N. El-Qada, S.J. Allen, G.M. Walker, Adsorption of basic dyes from aqueous solution onto activated carbons, Chem. Eng. J. 135 (2008) 174–184.
[4] B.H. Hameed, A.L. Ahmad, K.N.A. Latiff, Adsorption of basic dye (methylene blue) onto activated carbon prepared from rattan sawdust, Dyes Pigments 75 (2007) 143–149.
[5] S.M. Sidik, A.A. Jalil, S. Triwahyono, S.H. Adam, M.A.H. Satar, B.H. Hameed, Modified oil palm leaves adsorbent with enhanced hydrophobicity for crude oil removal, Chem. Eng. J. 203 (2012) 9–18.
[6] A.A. Jalil, S. Triwahyono, M.R. Yaakob, Z.Z.A. Azmi, N. Sapawe, N.H.N. Kamarudin, H.D. Setiabudi, N.F. Jaafar, S.M. Sidik, S.H. Adam, B.H. Hameed, Utilization of bivalve shell-treated *Zea mays* L. (maize) husk leaf as a low-cost biosorbent for enhanced adsorption of malachite green, Bioresour. Technol. 120 (2012) 218–224.
[7] E. Bulut, M. Ozacar, I.A. Sengil, Equilibrium and kinetic data and process design for adsorption of Congo Red onto bentonite, J. Hazard. Mater. 154 (2008) 613–622.
[8] C.C. Wang, L.C. Juang, T.C. Hsu, C.K. Lee, F.C. Huang, Adsorption of basic dyes onto montmorillonite, J. Colloid Interface Sci. 273 (2004) 80–86.
[9] M.H. Karaoglu, M. Dogan, M. Alkan, Removal of cationic dyes by kaolinite, Microporous Mesoporous Mater. 122 (2009) 20–27.
[10] R. Han, Y. Wang, Q. Sun, L. Wang, J. Song, X. He, C. Dou, Malachite green adsorption onto natural zeolite and reuse by microwave irradiation, J. Hazard. Mater. 175 (2010) 1056–1061.
[11] S.J. Allen, E. Ivanova, B. Koumanova, Adsorption of sulfur dioxide on chemically modified natural clinoptilolite. Acid modification, Chem. Eng. J. 152 (2009) 389–395.
[12] B.A. Shah, A.V. Shah, R.V. Tailor, Equilibrium, kinetics and breakthrough curve of phenol sorption on zeolitic material derived from BFA, J. Disper. Sci. Technol. 33 (2012) 41–51.
[13] B.A. Shah, C.B. Mistry, A.V. Shah, Sequestration of Cu(II) and Ni(II) from wastewater by synthesized zeolitic materials: equilibrium, kinetics and column dynamics, Chem. Eng. J. 220 (2013) 172–184.
[14] A.S. Ozcan, B. Erdem, A. Ozcan, Adsorption of Acid Blue 193 from aqueous solutions onto BTMA-bentonite, Colloids Surf. A: Physicochem. Eng. Asp. 266 (2005) 73–81.
[15] N. Kuanchertchoo, S. Kulprathiapanja, P. Aungkavattana, D. Atong, K. Hemra, T. Rirksomboon, S. Wongkasemjit, Preparation of uniform and nano-sized NaA zeolite using silatrane and alumatrane precursors, Appl. Organomet. Chem. 20 (2006) 775–783.
[16] A. Huang, W. Yang, Hydrothermal synthesis of NaA zeolite membrane together with microwave heating and conventional heating, Mater. Lett. 61 (2007) 5129–5132.
[17] W. Yuan, H. Chen, R. Chang, L. Li, Synthesis and characterization of NaA zeolite particle as intumescent flame retardant in chloroprene rubber system, Particualogy 9 (2011) 248–252.
[18] P.M. Slangen, J.C. Jansen, H. van Bekkum, The effect of ageing on the microwave synthesis of zeolite NaA, Microporous Mater. 9 (1997) 259–265.
[19] A. Ozer, G. Gurbuz, A. Calimli, B.K. Korbahti, Investigation of nickel (II) biosorption on *Enteromorpha prolifera*: optimization using response surface analysis, J. Hazard. Mater. 152 (2008) 778–788.
[20] B.K. Tiwari, K. Muthukumarappan, C.P.O. Donnell, P.J. Cullen, Modelling colour degradation of orange juice by ozone treatment using response surface methodology, J. Food Eng. 88 (2008) 553–560.
[21] Y. Zhou, B. Zhang, X. Zhang, J. Wang, J. Liu, R. Chen, Preparation of highly ordered cubic NaA zeolite from halloysite mineral for adsorption of ammonium ions, J. Hazard. Mater. 178 (2010) 658–664.
[22] A.R. Loila, J.C.R.A. Andrade, J.M. Sasaki, L.R.D. da Silva, Structural analysis of zeolite NaA synthesized by a cost-effective hydrothermal method using kaolin and its use as water softener, J. Colloid Interface Sci. 367 (2012) 34–39.
[23] M.J.K. Bashir, H.A. Aziz, M.S. Yusoff, M.N. Adlan, Application of response surface methodology (RSM) for optimization of ammoniacal nitrogen removal from semi-aerobic landfill leachate using ion exchange resin, Desalination 254 (2010) 154–161.
[24] D. Nibou, S. Khemaissia, S. Amokrane, M. Barkat, S. Chegrouche, A. Mellah, Removal of UO_2^{2+} onto synthetic NaA zeolite. Characterization, equilibrium and kinetic studies, Chem. Eng. J. 172 (2011) 296–305.
[25] B.H. Hameed, Removal of cationic dye from aqueous solution using jackfruit peel as non-conventional low-cost adsorbent, J. Hazard. Mater. 162 (2009) 344–350.
[26] A.B. Albadarin, C. Mangwandi, A.H. Al-Muhtaseb, G.M. Walker, S.J. Allen, M.N.M. Ahmad, Kinetic and thermodynamics of chromium ions adsorption onto low-cost dolomite adsorbent, Chem. Eng. J. 179 (2012) 193–202.
[27] M. Auta, B.H. Hameed, Modified mesoporous clay adsorbent for adsorption isotherm and kinetics of methylene blue, Chem. Eng. J. 198–199 (2012) 219–227.
[28] A.A. Jalil, S. Triwahyono, S.H. Adam, N.D. Rahim, M.A.A. Aziz, N.H.H. Hairom, N.A.M. Razali, M.A.Z. Abidin, M.K.A. Mohamadiah, Adsorption of methyl orange from aqueous solution onto calcined Lapindo volcanic mud, J. Hazard. Mater. 181 (2010) 755–762.
[29] J. Anwar, U. Shafique, M. Salman, S. Waheed-uz-Zaman, J.M. Anwar, Anzano, Removal of chromium(III) by using coal as adsorbent, J. Hazard. Mater. 171 (2009) 797–801.
[30] S.T. Akar, A. Gorgulu, Z. Kaynak, B. Anilan, T. Akar, Biosorption of Reactive Blue 49 dye under batch and continuous mode using a mixed biosorbent of macrofungus *Agaricus bisporus* and *Thuja orientalis* cones, Chem. Eng. J. 148 (2009) 26–34.
[31] A. Gurses, C. Dogar, M. Yalcin, M. Acikyildiz, R. Bayrak, S. Karaca, The adsorption kinetics of the cationic dye, methylene blue, onto clay, J. Hazard. Mater. B131 (2006) 217–228.
[32] B.A. Shah, A.V. Shah, H.D. Patel, Alkaline hydrothermal conversion of agricultural waste bagasse fly ash into zeolitic: utilization in dye removal from aqueous solutions, Int. J. Environ. Waste Manage. 7 (2011) 192–208.
[33] C. Woolard, J. Strong, C. Erasmus, Evaluation of the use of modified coal ash as a potential sorbent for organic waste streams, Appl. Geochem. 17 (2002) 1159–1164.
[34] D. Ghosh, K.G. Bhattacharyya, Adsorption of methylene blue on kaolinite, Appl. Clay Sci. 20 (2002) 295–300.
[35] D. Kavitha, C. Namasivayam, Experimental and kinetic studies on methylene blue adsorption by coir pith carbon, Bioresour. Technol. 98 (2007) 14–21.
[36] S. Arivoli, M. Hema, S. Parthasarathy, P. Manju, Adsorption dynamics of methylene blue by acid activated carbon, J. Chem. Pharm. Res. 2 (2010) 626–641.

[37] O. Gercel, A. Ozcan, A.S. Ozcan, H.F. Gercel, Preparation of activated carbon from a renewable bio-plant of *Euphorbia rigida* by H_2SO_4 activation and its adsorption behaviour in aqueous solutions, Appl. Surf. Sci. 253 (2007) 4843–4852.
[38] M. Alaya, M. Hourieh, A. Youssef, F. El-Sejarah, Adsorption properties of activated carbons prepared from olive stones by chemical and physical activation, Adsorp. Sci. Technol. 18 (1999) 27–42.
[39] C. Sainz-Diaz, A. Griffiths, Activated carbon from solid wastes using a pilot-scale batch flaming pyrolyser, Fuel 79 (2000) 1863–1871.
[40] C. Lee, K. Low, S. Chow, Chrome sludge as an adsorbent for color removal, Environ. Technol. 17 (1996) 1023–1028.
[41] L.S. Oliveira, A.S. Franca, T.M. Alves, S.D.F. Rocha, Evaluation of untreated coffee husks as potential biosorbents for treatment of dye contaminated waters, J. Hazard. Mater. 155 (2008) 507–512.
[42] K.V. Kumar, K. Porkodi, Relation between some two- and three-parameter isotherm models for the sorption of methylene blue onto lemon peel, J. Hazard. Mater. 138 (2006) 633–635.
[43] G. Annadurai, R. Juang, D. Lee, Use of cellulose-based wastes for adsorption of dyes from aqueous solutions, J. Hazard. Mater. 92 (2002) 263–274.
[44] F.A. Pavan, E.C. Lima, S.L.P. Dias, A.C. Mazzocato, Methylene blue biosorption from aqueous solutions by yellow passion fruit waste, J. Hazard. Mater. 150 (2008) 703–712.
[45] H. Demir, A. Top, D. Balkose, S. Ulku, Dye adsorption behavior of *Luffa cylindrical* fibers, J. Hazard. Mater. 153 (2008) 389–394.
[46] M.A.Z. Abidin, A.A. Jalil, S. Triwahyono, S.H. Adam, N.H.N. Kamarudin, Recovery of gold (III) from an aqueous solution onto a *durio zibethinus* husk, Biochem. Eng. J. 54 (2011) 124–131.
[47] Y.-S. Ho, W.-T. Chiu, C.-C. Wang, Regression analysis for the sorption isotherms of basic dyes on sugarcane dust, Bioresour. Technol. 96 (2005) 1285–1291.
[48] W.T. Chen, C.W. Lin, P.K. Shih, W.L. Chang, Adsorption of phosphate into waste oyster shell: thermodynamic parameters and reaction kinetics, Desalin. Water Treat. 47 (2012) 86–95.
[49] Z. Belala, M. Jeguirim, M. Belhachemi, F. Addoun, G. Trouve, Biosorption of basic dye from aqueous solutions by date stones and palm-trees waste: kinetic, equilibrium and thermodynamic studies, Desalination 271 (2011) 80–87.
[50] Y. Zhang, W. Shi, H. Zhou, X. Fu, X. Chen, Kinetic and thermodynamic studies on the adsorption of anionic surfactant on quaternary ammonium cationic cellulose, Water Environ. Res. 82 (2010) 567–573.
[51] N. Sapawe, A.A. Jalil, S.H. Adam, N.F. Jaafar, M.A.H. Satar, Isomorphous substitution of Zr in the framework of aluminosilicate HY by an electrochemical method: Evaluation by methylene blue decolorization, Appl. Catal. B: Environ. 125 (2012) 311–323.
[52] N.F. Jaafar, A.A. Jalil, S. Triwahyono, M.N.M. Muhid, N. Sapawe, M.A.H. Satar, H. Asaari, Photodecolorization of methyl orange over α-Fe_2O_3-supported HY catalysts: the effects of catalyst preparation and dealumination, Chem. Eng. J. 191 (2012) 112–122.
[53] N. Sapawe, A.A. Jalil, S. Triwahyono, R.N.R.A. Sah, N.W.C. Jusoh, N.H.H. Hairom, J. Efendi, Electrochemical strategy for grown ZnO nanoparticles deposited onto HY zeolite with enhanced photodecolorization of methylene blue: effect of the formation of Si–O–Zn bonds, Appl. Catal. A: Gen. 456 (2013) 144–158.
[54] N. Sapawe, A.A. Jalil, S. Triwahyono, One-pot electro-synthesis of ZrO_2–ZnO/HY nanocomposite for photocatalytic decolorization of various dye-contaminants, Chem. Eng. J. 225 (2013) 254–265.
[55] M. Huang, C. Xu, Z. Wu, Y. Huang, J. Lin, J. Wu, Photocatalytic discolorization of methyl orange solution by Pt modified TiO_2 loaded on natural zeolite, Dyes Pigments 77 (2008) 327–334.
[56] B.A. Shah, A.V. Shah, H.D. Patel, Equilibrium and kinetic studies of the adsorption of basic dye from aqueous solutions by zeolite synthesized from bagasse fly ash, Environ. Prog. Sustain. Energy 30 (2011) 549–557.